Induced electron transfer by oxygen vacancy gradient on SnO₂ conductive glass for electrocatalytic reduction

Xiaoyun Zhang[†], Dong Li[†], Lian Wang, Fan Yang and Yuqiao Wang[*]

Interface engineering is a strategy to boost intrinsic catalytic activities. Defect introduction, composition regulation, and heterostructure engineering are commonly used interface modification methods [1,2]. Oxygen vacancy (O_V) modulates electronic properties and structures by controlling surface electronic and atomic structures [3–5]. O_V is common to metal oxides (MOxs) as a shallow donor due to low formation energy [6,7]. It plays an essential role in many photoelectrochemical (PEC) processes, such as PEC water splitting, dye-sensitized solar cells (DSSCs), supercapacitors, lithium-ion batteries (LIBs), and CO_2 electro-reduction [8,9]. At present, methods for regulating O_V include plasma treatment, ambient annealing of oxygen defects, flame reduction, laser ablation, and electrochemical reduction [10,11].

Simulations and experiments reveal the effect of O_V on the electrocatalytic (EC) performance [12]. O_V can change the electronic structure of MOxs and affect the electron transport rate in the EC process [13]. F-doped tin oxide (FTO) conductive glass is commonly used in PEC devices [14]. The main component of FTO surface coating is tin dioxide (SnO_2), a wide bandgap MOx, which has been widely used in ceramic glass, LIB, and conductive glass coating industries [15–17]. The surface O_V in MOxs tuning electronic structure is expected to control the electron transfer direction, thereby promoting the EC reaction [18,19]. Inspired by this, we constructed O_V concentration gradient on FTO as a counter electrode (CE) in DSSCs to promote electron enrichment on the FTO surface, thus increasing the EC reduction rate of triiodide ions.

We calculated the O_V distribution on the SnO_2 surfaces theoretically and designed an EC reduction reaction to verify the hypothesis. Theoretically, rutile SnO_2 based on lattice constants (a = 4.7373 Å and c = 3.1864 Å) and bandgap (3.6 eV) was used to build (110) surface, which was modeled by p (3×2) periodically repeated slabs. The electronic properties of rutile SnO_2 were investigated *via* the first principles in the framework of density functional theory. The calculations were performed within generalized gradient approximation using projector-augmented wave pseudopotentials, as implemented in Vienna *Ab initio* Simulation Package. The energy cutoff for plane-wave basis was set to 450 eV. The atomic positions relaxed until forces on each atom were less than 0.01 eV Å^{-1}. The self-consistent convergence accuracy was set to 10^{-5} eV. A typical EC reduction from triiodide (I_3^-) to iodide (I^-) on CE surfaced in DSSCs. The ideal CE had a powerful ability to collect external electrons for rapid reduction. Therefore, as a model reaction, the EC reduction was employed to verify the electron transfer direction under tuning surface O_V concentration gradient of SnO_2.

Each slab contained five trilayers and a vacuum space of 10 Å along the z-direction (Fig. 1a). The atoms of the left two layers were fixed at their bulk positions. Three-fold coordination of oxygen atoms reduced to two folds on the surface. Two-fold O atoms on the surface (O_{2c}) and three-fold O atoms in bulk (O_{bulk}) were used to simulate the possible presence of O_V after air insulation heat treatment. The surface electrostatic potential was averaged in the x–y plane perpendicular to the z-direction (Fig. 1b). The vacuum potentials (E_{vac}) from both normal and defective surfaces were treated as identical numerically, which would act as reference energies for aligning Kohn–Sham levels of different surfaces.

Fig. 2a shows the calculated energy positions of conduction and valence band edges. The shifts in band edges

Institute of Advanced Materials, School of Chemistry and Chemical Engineering, Southeast University, Nanjing 211189, China
[†] These authors contributed equally to this work.
[*] Corresponding author (email: yqwang@seu.edu.cn)
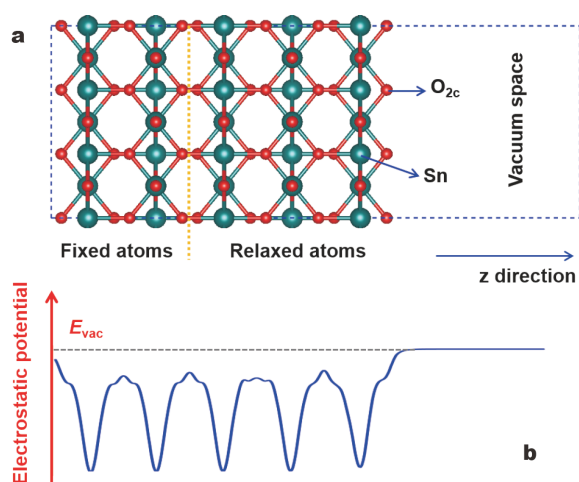
**Figure 1** (a) Side view of rutile SnO_2 (110) surface with surface defect O_V; (b) vacuum potentials from normal and defective surfaces of SnO_2.

of the rutile SnO_2 (110) were induced by the presence of surface O_V due to the annealed SnO_2. The bottom of open circles and the top of solid circles represent the conduction and valence band edges, respectively. The formation energy of O_{2c} vacancies was 0.81 eV less than that of O_{bulk} vacancies. The result indicates that O_{2c} vacancies could cause more shifts of band edges of the host surface than those of O_{bulk} vacancies. The certain vacancy concentration leads to stronger reduction power of electrons in the conduction band of SnO_2 (Fig. 2b), which could not influence the flow of electrons from the conduction band of TiO_2 to that of SnO_2. Increasing vacancy concentrations would cause a higher shift of SnO_2 conduction band edge than that of TiO_2, thus blocking the flow of electrons back to SnO_2 (Fig. 2c). Therefore, the appropriate operation of vacancy concentration could effectively regulate the efficiency of electron injection. The results of this optimization were also confirmed by subsequent catalytic experiments (Fig. 2d). The maximum value of photoelectric conversion efficiency was obtained after 10-min annealing treatment. Hence, we started with a theoretical explanation that surface O_V gradient revealed the influence of O_V on the band structure and their relationship using an experimental technique (Fig. 2e).

SnO_2 without any treatment, as a pure semiconductor, exhibited the general characteristics of electron transfer. After heating, the O_V concentration on the SnO_2 surface began to change, thereby inducing a change in the electron transfer. O_V concentration approximately increased proportionally with the heating time. With the increase in heating time, the surface O_V started diffusing from the surface to bulk phase, whereas the number of surface

vacancies decreased. Therefore, the SnO_2 band bending demonstrated downward bending, horizontal downward shifting, and upward bending due to the O_V concentration and distribution. The band edge position was beneficial to the spontaneous enrichment of electrons on the SnO_2 surface when surface O_V concentration was balanced with the bulk O_V concentration. Therefore, this process can be used to tune the electron transfer direction by manipulating experimental conditions to control the O_V concentration and distribution.

FTO substrate was annealed at 550°C under air insulation heat treatment with a vacuum of 0.01 Pa to form O_V–SnO_2 on the FTO surface. The result was monitored *via* electron paramagnetic resonance (EPR) spectrum (Fig. S1), referring to the peak at 325 Gauss as fingerprint evidence for probing O_V [20]. The O_V occurred when the titanium sheet, as a substrate for coating SnO_2, underwent the same heat treatment (Fig. 3a). The SnO_2/Ti substrate annealed in isolated air had an obvious vacancy response, whereas the SnO_2 annealed in filled air had no response, which means that SnO_2 could generate O_V after heat treatment under low-pressure conditions without air. Surface O_V was unrelated to fluorine dopants. This processing method effectively formed O_V and was confirmed by Raman spectroscopy (Fig. 3b). The distribution gradient of O_V was expressed by the corresponding intensities of Raman spectra; it was closely related to the heating time. The effect of heating time on the SnO_2 crystalline was insignificant. The characteristic diffraction peaks at 26.6°, 33.9°, 38.0°, 51.8°, 54.7°, and 57.9° correspond to the (110), (101), (200), (211), (220), and (002) planes of SnO_2, respectively (JCPDS No. 70-4177) (Fig. S2).

The heat-treated FTO was used as a CE to assemble DSSCs. The properties of FTO CEs were evaluated by the device performance (Fig. S3), including photocurrent density–voltage curves, cyclic voltammetry (CV), and Tafel polarization curves (Table S1). The short circuit current density (J_{SC}) first increased and then decreased with prolonging the heating time of FTO treatments using Pt as a reference CE. The FTO treated for 10 min (FTO-10 min) yielded J_{SC} of 9.35 mA cm^{-2}, V_{OC} of 0.79 V and fill factor of 0.60. The current density was mainly determined by the catalytic rate on the CE surface. The J_{SC} values of DSSCs based on various CEs followed the order: Pt > FTO-10 min > FTO-5 min > FTO-30 min > FTO-50 min. Further, the high cathodic peak current density (J_{PC}) and low peak to peak separation (E_{PP}) reflected good EC reduction from I_3^- to I^- in the CV curves. The pair of redox peaks corresponded to the oxidation
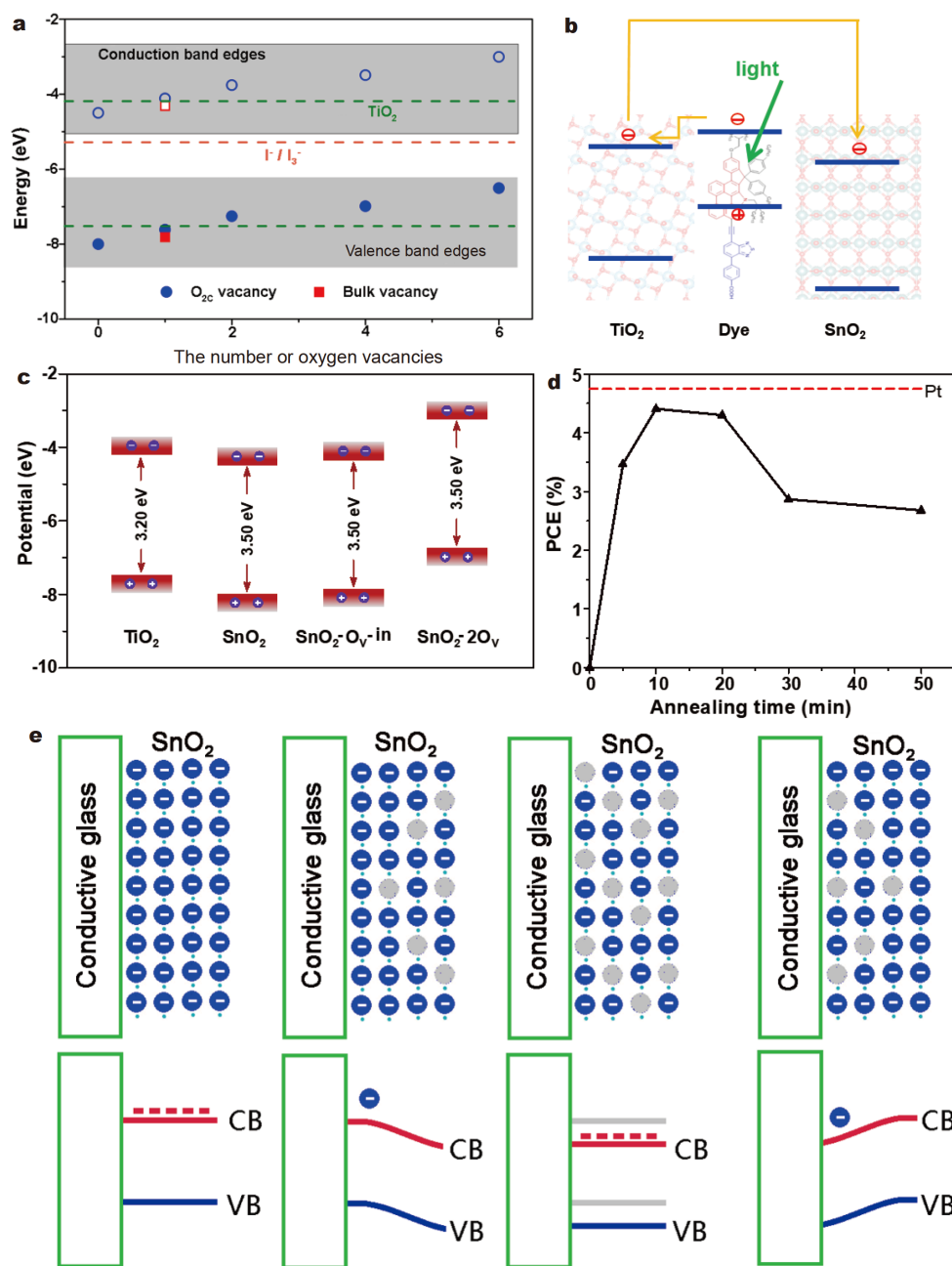
Figure 2 (a) Calculated energy positions of the conduction and valence band edges of the annealed SnO_2; (b, c) band position schematic of TiO_2, SnO_2, SnO_2–O_V–in, and SnO_2–$2O_V$; (d) PCE of annealed SnO_2 with different annealing times; (e) concentration gradient of O_V on SnO_2 surface with different annealing times.

and reduction of I^-/I_3^- in the low potential region. The rate-determining step was decided by the reduction from I_3^- to I^-. The other pair of redox reactions (I^-/I_3^-) belonged to a fast equilibrium in the high potential region. Owing to the same reason as J_{PC}, the trend of exchange current density (J_0) was identified with Tafel polarization. The reversibility of FTO-10 min was almost comparable

to that of Pt, although the E_{PP} value was slightly higher.

Generally, a surface catalysis process is mainly affected by the concentration and distribution of the catalysts. By that analogy, EC reduction from I_3^- to I^- was determined by the O_V concentration and distribution. In our report, the heat treatment atmosphere, air pressure, and heating time had direct effects on the O_V concentration and
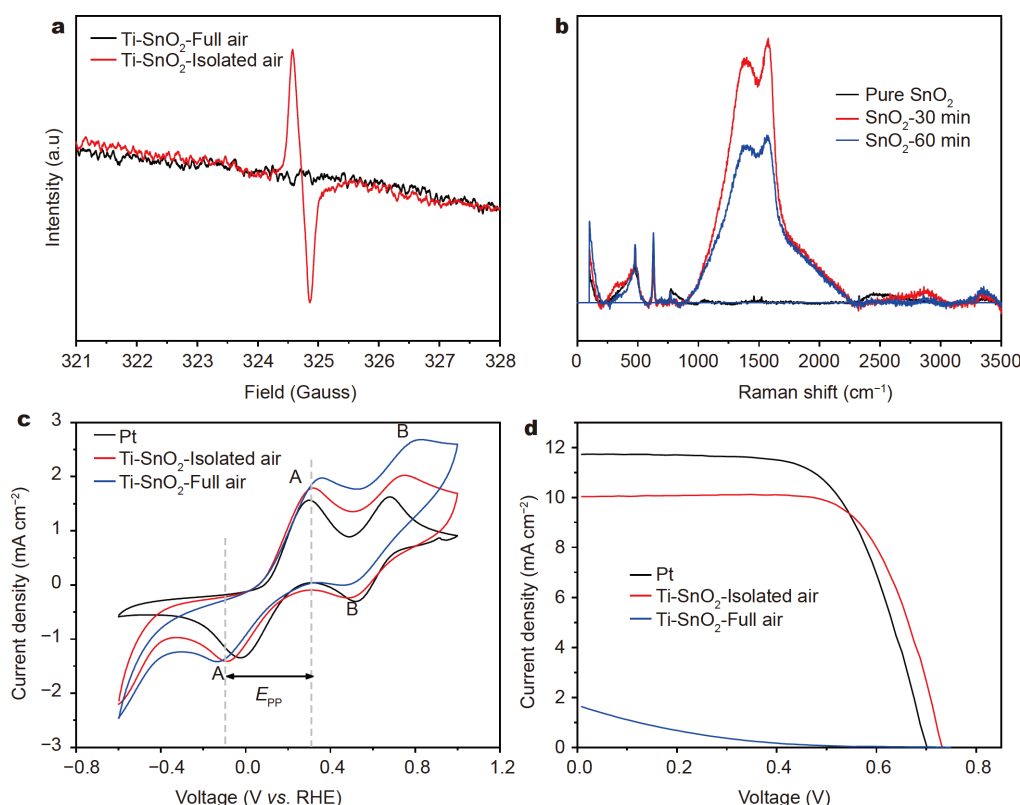
Figure 3 (a) Electron paramagnetic resonance spectra of the SnO_2 annealed in isolated and full air. (b) Raman spectra of SnO_2 with different annealing times. (c) CV curves of Pt and SnO_2 electrode with Ti substrate. (d) Photocurrent density–voltage curves of DSSCs based on SnO_2 counter electrode with Ti substrate.

distribution. High-temperature treatment could effectively produce O_V under isolated air and low pressure. With the extension of the heating time, the concentration of O_V increased from low to high, and the distribution was from the surface to the inside, which agreed with previous theoretical simulation and was proven experimentally. This method for producing O_V on the SnO_2 surface can also be used for other substrates. O_V–SnO_2/Ti substrate also showed catalytic performance similar to that of O_V–FTO, including CV (Fig. 3c) and device performance (Fig. 3d).

In summary, heat treatment of SnO_2 is an effective method to create O_V under isolated air and low pressure. Their concentration and distribution can be tuned by heating time. The surface O_V of SnO_2 can improve the efficiency of EC reduction reactions.

1   Wang J, Zhang Z, Ding J, et al. Recent progresses of micro-nanostructured transition metal compound-based electrocatalysts for energy conversion technologies. Sci China Mater, 2021, 64: 1–26

2   Fang HX, Guo H, Niu CG, et al. Hollow tubular graphitic carbon nitride catalyst with adjustable nitrogen vacancy: Enhanced optical absorption and carrier separation for improving photocatalytic activity. Chem Eng J, 2020, 402: 126185

3   Yang L, Liu R, Jiao L. Electronic redistribution: construction and modulation of interface engineering on CoP for enhancing overall water splitting. Adv Funct Mater, 2020, 30: 1909618

4   Zhang Y, Tao L, Xie C, et al. Defect engineering on electrode materials for rechargeable batteries. Adv Mater, 2020, 32: 1905923

5   Wang G, Yang Y, Han D, et al. Oxygen defective metal oxides for energy conversion and storage. Nano Today, 2017, 13: 23–39

6   Zhuang G, Chen Y, Zhuang Z, et al. Oxygen vacancies in metal oxides: recent progress towards advanced catalyst design. Sci China Mater, 2020, 63: 2089–2118

7   Shao C, Malik AS, Han J, et al. Oxygen vacancy engineering with flame heating approach towards enhanced photoelectrochemical water oxidation on WO_3 photoanode. Nano Energy, 2020, 77: 105190

8   Shao Z, Sun J, Guo N, et al. Boosting electrocatalysis by heteroatom doping and oxygen vacancies in hierarchical Ni-Co based nitride phosphide hybrid. J Power Sources, 2019, 422: 33–41

9   Liu Z. Highly efficient electroreduction of carbon dioxide to formate over copper dendrites derived from in situ electrosynthesized coppermetal-oxide frameworks. Acta Physico Chim Sin, 2020, 36: 2006006

10 Zhu C, Li C, Zheng M, et al. Plasma-induced oxygen vacancies in

ultrathin hematite nanoflakes promoting photoelectrochemical water oxidation. ACS Appl Mater Interfaces, 2015, 7: 22355–22363

11 Meng C, Lin M, Sun X, et al. Laser synthesis of oxygen vacancy-modified CoOOH for highly efficient oxygen evolution. Chem Commun, 2019, 55: 2904–2907

12 Shi L, Yin Y, Wang S, et al. Rigorous and reliable operations for electrocatalytic nitrogen reduction. Appl Catal B-Environ, 2020, 278: 119325

13 Bi W, Ye C, Xiao C, et al. Spatial location engineering of oxygen vacancies for optimized photocatalytic H_2 evolution activity. Small, 2014, 10: 2820–2825

14 Morales DM, Kazakova MA, Dieckhöfer S, et al. Trimetallic Mn-Fe-Ni oxide nanoparticles supported on multi-walled carbon nanotubes as high-performance bifunctional ORR/OER electrocatalyst in alkaline media. Adv Funct Mater, 2020, 30: 1905992

15 Basu K, Selopal GS, Mohammadnezad M, et al. Hybrid graphene/metal oxide anodes for efficient and stable dye sensitized solar cell. Electrochim Acta, 2020, 349: 136409

16 Zhou X, Yu L, Lou XWD. Formation of uniform N-doped carbon-coated SnO_2 submicroboxes with enhanced lithium storage properties. Adv Energy Mater, 2016, 6: 1600451

17 Zhou X, Wan LJ, Guo YG. Binding SnO_2 nanocrystals in nitrogen-doped graphene sheets as anode materials for lithium-ion batteries. Adv Mater, 2013, 25: 2152–2157

18 Han H, Jin S, Park S, et al. Plasma-induced oxygen vacancies in amorphous MnO_x boost catalytic performance for electrochemical CO_2 reduction. Nano Energy, 2020, 79: 105492

19 Mo S, Zhang Q, Li J, et al. Highly efficient mesoporous MnO_2 catalysts for the total toluene oxidation: Oxygen-vacancy defect engineering and involved intermediates using in situ DRIFTS. Appl Catal B-Environ, 2020, 264: 118464

20 Wang Q, Liu Z, Liu D, et al. Ultrathin two-dimensional $BiOBr_xI_{1-x}$ solid solution with rich oxygen vacancies for enhanced visible-light-driven photoactivity in environmental remediation. Appl Catal B-Environ, 2018, 236: 222–232

Author contributions All authors listed have made a direct and intellectual contribution to the work, and approved it for publication.

Conflict of interest The authors declare no conflict of interest.

Supplementary information Experimental details and supporting data are available in the online version of the paper.

Xiaoyun Zhang is currently a PhD candidate in the Nano Photo-electrochemistry & Device Group, at the Southeast University, under the supervision of Prof. Yuqiao Wang. She received her BSc (2017) and MSc (2020) degrees from China University of Mining and Technology. Her research interests focus on the development of high-efficiency catalysis and the electrocatalytic mechanism of electrocatalytic reduction reaction.

Dong Li is currently a Master candidate in the Nano Photo-electrochemistry & Device Group at the Southeast University, under the supervision of Prof. Yuqiao Wang. He received his BSc degree in chemical engineering in 2019 from Anqing Normal University. His current research focuses on the development of high-efficiency catalysis for water-splitting.

Yuqiao Wang received his BSc degree in fine chemicals (2001) from Anhui University, and MSc (2005) and PhD (2008) degrees in material physics & chemistry from the Southeast University. Now, he is a Full Professor at the Southeast University, who is also the Head of Nano Photo-electrochemistry & Device Group. His current research interests include the design and synthesis of nanostructured photoelectrochemical functional materials, the related device integration, and the relationship between material invalidation and device performance attenuation.

氧空位浓度梯度诱导电子转移的电催化还原

张晓云†, 李东†, 王练, 杨帆, 王育乔*

摘要 通过表面氧空位缺陷调控催化剂的表面电子结构, 实现催化剂表面易于富集参与反应的电子, 从而提高还原催化效率. 本文中, 将导电玻璃隔绝空气加热, 在其表面形成氧空位缺陷. 通过控制热处理时间调控表面氧空位浓度梯度. 氧空位能导致SnO_2导带弯曲, 因此调控氧空位梯度可增强SnO_2导电玻璃表面电子富集速率, 从而实现高效电催化还原反应. 在相同条件下, 使其催化性能可以和金属铂相媲美.